Cyclic Tests of
Long Shear Walls with Openings

Virginia Polytechnic Institute and State University
Department of Wood Science and Forests Products
Brooks Forest Products Research Center
Timber Engineering Center
1650 Ramble Road
Blacksburg, Virginia 24061-0503

Report No. TE-1996-002

by:

J.D. Dolan
Associate Professor of Wood Engineering

A.C. Johnson
Research Assistant

June 20, 1997

INTRODUCTION

Wood frame shear walls are a primary lateral force resisting element in wood frame structures. Traditional shear wall design requires fully sheathed wall sections restrained against overturning. Their behavior is often considered analogous to a deep cantilever beam with the end framing members acting as "flanges" or "chords" to resist overturning moment forces and the panels acting as a "web" to resist shear. This analogy is generally considered appropriate for wind and seismic design. Overturning and shear restraint, and chord forces are easily calculated using principles of engineering mechanics. While shear resistance can be calculated as well, tabulated shear resistance's for varying fastener schedules are often used.

Traditional design of exterior shear walls containing openings, for windows and doors, involves the use of multiple shear wall segments. Each is required to be fully sheathed and have overturning restraint supplied by structure weight and/or mechanical anchors. The design capacity of shear walls is assumed to equal the sum of the capacities for each shear wall segment. Sheathing above and below openings is typically not considered to contribute to the overall performance of the wall.

An alternate empirical-based approach to the design of shear walls with openings is the perforated shear wall method which appears in the *Standard Building Code 1996 Revised Edition* and the *Wood Frame Construction Manual for One- and Two- Family Dwellings - 1995 High Wind Edition.* The perforated shear wall method consists of a combination of prescriptive provisions and empirical adjustments to design values in shear wall selection tables for the design of shear wall segments containing openings. When designing for a given load, shear walls resulting from this method will have a reduced number of overturning restraints than a similar shear wall constructed with multiple traditional shear wall segments.

A significant number of monotonic tests of one-third scale models and shorter full-sized walls provide verification of the perforated shear wall method. This study provides additional information about the performance of long, full-sized, perforated shear walls tested under monotonic and cyclic loads. Cyclic tests are performed to establish conservative estimates of performance during a seismic event. Results of cyclic tests are presented in this report (TE-1996-002) and monotonic test results are reported in Dolan and Johnson (1996) (TE-1996-001). A detailed description and discussion of the complete investigation is presented in Johnson (1997).

OBJECTIVES

Results of an experimental study of the performance of shear walls meeting the requirements of the perforated shear wall method are reported. The objectives of this study were 1) determine the effects of openings on full-size wood frame shear walls tested monotonically and cyclically, 2) determine if the perforated shear wall method conservatively predicts capacity.

BACKGROUND

The perforated shear wall design method appearing in the *Standard Building Code 1996 Revised Edition (SBC)* and the *Wood Frame Construction Manual for One- and Two- Family Dwellings - 1995 High Wind Edition (WFCM)* is based on an empirical

equation which relates the strength of a shear wall segment with openings to one without openings. The empirical equation developed by Sugiyama (1993) forms the basis of adjustment factors in Table 2313.2.2 in the SBC and Supplement Table 3B in the WFCM. Tabulated adjustment factors are used to reduce the strength of a traditional fully sheathed shear wall segment for the presence of openings.

In accordance with SBC and WFCM, and for the purposes of this study, a perforated shear wall must have: 1) mechanical overturning and shear restraint; 2) tie-downs to provide overturning restraint and maintain a continuous load path to the foundation where any plan discontinuities occur in the wall line; 3) minimum length of full-height sheathing at each end of the wall (Based on height-to-length ratios for blocked shear wall segments as prescribed by the applicable building code.); 4) maximum ultimate shear capacity of less than or equal to 1500 plf.

Prescriptive provisions and empirical adjustments are based on parameters of various studies conducted on shear walls with openings. Many of the prescriptive provisions are necessary to meet conditions for which walls in previous studies were tested. Empirically derived adjustment factors, or shear capacity ratios, for the perforated shear wall method are based on an equation developed by Sugiyama (1994) for predicting shear capacity ratios.

The shear capacity ratio, or the ratio of the strength of a shear wall segment with openings to the strength of a fully sheathed shear wall segment without openings, is determined by Equation (1):

$$F = r / (3 - 2 \cdot r) \tag{1}$$

where 'F' is shear capacity ratio and 'r' is the sheathing area ratio.

Sheathing area ratio is used to classify walls based on the size of openings present. It is determined by: a) the ratio of the area of openings to the area of wall and b) the length of wall with full height sheathing to the total length of the wall. Sheathing area ratio parameters are illustrated in Figure 1, and the ratio can be calculated by the following expression:

$$r = \frac{1}{(1 + \dfrac{\alpha}{\beta})} \tag{2}$$

$$\alpha = \frac{\text{Area of openings}}{H \cdot L} \tag{3}$$

$$\beta = \frac{\sum L_i}{L} \tag{4}$$

where α = opening area ratio,
        β = wall length ratio,

ΣL_i =   sum of the length of full height sheathing,

L   =   shear wall length, and
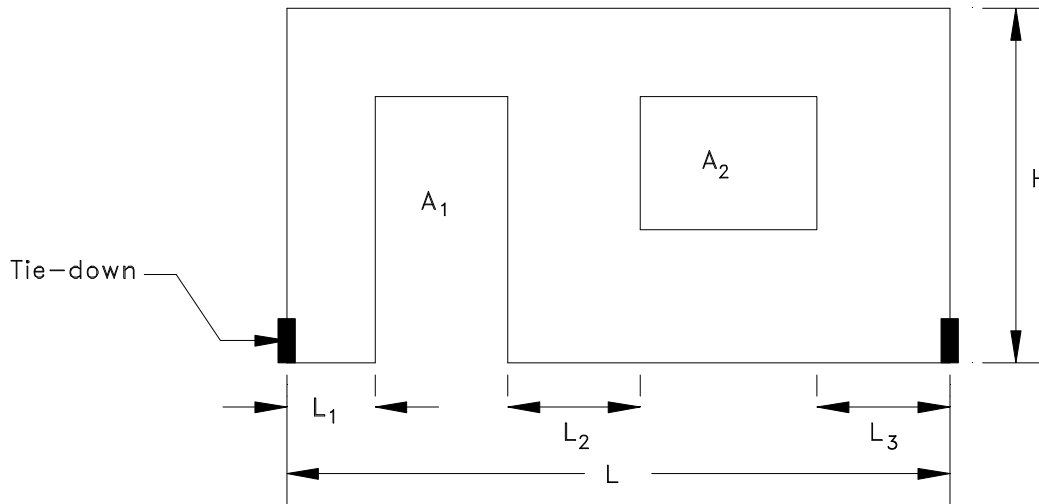
H   =   wall height.

Figure 1: Sheathing area ratio variables

Tabulated shear capacity ratios or opening adjustment factors appearing in the SBC and WFCM are based on Equation (1) assuming that the height of all openings in a wall are equal to the largest opening height. The result is that SBC and WFCM tabulated shear capacity ratios or opening adjustment factors for walls containing openings of varying height are smaller than would be calculated using Equation (1). For this study, Equation (1) will be used to predict the performance of shear walls with openings constructed in accordance with the parameters of the perforated shear wall design method. Tabulated shear capacity ratios appearing in the SBC and WFCM result in slightly more conservative estimates of performance.
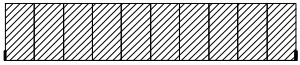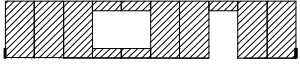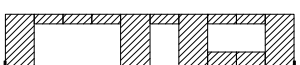
TEST PROGRAM

Monotonic and cyclic tests were conducted on pairs of walls for each of the five wall configurations shown in Table 1. Size and placement of openings was selected to cover the range of sheathing area ratios, 'r', encountered in light wood frame construction. Perforated shear wall performance under monotonic and cyclic loads over the range of sheathing area ratios as well as a comparison between monotonic and cyclic performance is reported in this study. Results of cyclic tests are presented in this report (TE-1996-002) and monotonic test results are reported in Dolan and Johnson (1996) (TE-1996-001).

Specimen Configuration

Five 40 feet long by 8 feet tall walls were included in the cyclic investigation. Each wall used the same type of framing, sheathing, nails, and nailing patterns. Table 1 lists the opening dimensions and illustrates the opening locations for each wall configuration

included in the investigation. Wall A (r = 1.0) has no openings and is necessary for determining the capacity of the fully sheathed condition. The ratio of strength of Walls B through E to Wall A will be compared directly to the shear capacity ratio, F, calculated using Equation (1).

Table 1: Opening sizes for each wall configuration included in investigation

Wall Configuration[1]	Wall Type	Sheathing Area Ratio, (r)	Opening Size	
			Door	Window[2]
	A	1.0	-	-
	B	0.76	6'-8" x 4'-0"	5'-8" x 7'-10$\frac{1}{2}$"
	C	0.55	6'-8" x 4'-0"	4'-0" x 11'-10$\frac{1}{2}$" 4'-0" x 7'-10$\frac{1}{2}$"
	D	0.48	6'-8" x 4'-0" 6'-8" x 12'-0"	4'-0" x 7'-10$\frac{1}{2}$"
	E	0.30	(Sheathed at ends)[3] 8'-0" x 28'-0"	-

1: All walls are framed with studs spaced at 16 inches on center. Shaded areas represent sheathing.

2: The top of each window is located 16 inches from the top of the wall.

2: Wall E has studs along the full length of wall but is sheathed only at the ends of the wall.

Materials and Fabrication Details

Table 2 summarizes materials and construction details used for the wall specimens. Included are the size of headers and jack studs used around openings.

Wall framing consisted of double top plates, single bottom plates, double end studs, and double or triple studs around doors and windows. Studs were spaced 16 in. on center. All framing consisted of No. 2 grade spruce-pine-fir purchased from a local lumber yard. Members were arbitrarily chosen when placed in the wall specimens.

Exterior sheathing was 15/32 in., 4 ply, structural I plywood. All full height panels were 4 ft. by 8 ft. and oriented vertically. To accommodate openings, the plywood was cut to fit above and below the doors and windows.

Interior sheathing was 4 ft. by 8 ft. sheets of 1/2 in. gypsum wallboard, oriented vertically. As with plywood, the gypsum was cut to fit above and below the doors and windows. All joints in the interior sheathing were taped and covered with drywall compound. Taped joints were allowed to dry for a minimum of 3 days prior to testing.

Table 2: Wall materials and construction data

Component	Fabrication and Materials
Framing Members	No. 2, Spruce-Pine-Fir, 2 x 4 inch nominal
Sheathing:	
Exterior	Plywood, 15/32 in., 4 ply, Structural I. 4 ft. x 8 ft. sheets installed vertically.
Interior	Gypsum wallboard, 1/2 in., installed vertically, joints taped
Headers:	
4'-0" opening	(2) 2x4's with intermediate layer of 15/32 in. plywood. One jack stud at each end.
7'-10$\frac{1}{2}$" opening	(2) 2x8's with intermediate layer of 15/32 in. plywood. Two jack studs at each end.
11' - 10$\frac{1}{2}$" opening	(2) 2x12's with intermediate layer of 15/32 in. plywood. Two jack studs at each end.
Tie-down	Simpson HTT 22, nailed to end studs with 32 16d sinker nails. 5/8 in. diameter A307 bolt to connect to foundation.
Anchor Bolts	5/8 in. diameter A307 bolt with 3 in. square x 1/4 in. steel plate washers.

Both exterior and interior sheathing were able to rotate past the test fixture at the top and bottom (i.e. the steel test fixture was narrower than the wood framing used for top and bottom plates.)

Two tie-down anchors were used on each wall, one at each double stud at the ends of the wall specimens (approximately 40 feet apart.) Simpson Tie-down model HTT22 were used. Tie-down anchors were attached to the bottom of the end studs by thirty-two (32) 16d (0.148 in. diameter and 3.25 in. length) sinker nails. A 5/8 in. diameter bolt connected the tie-down, through the bottom plate, to the rigid structural steel tube test fixture.

Table 3 shows the fastener schedule used in constructing the wall specimens. Four different types of nails were used. 16d (0.162 in. diameter and 3.5 in. length) bright common nails connected the framing, 8d (0.131 in. diameter and 2.5 in. length) bright common nails attached the plywood sheathing to the frame, 16d (0.148 in. diameter and 3.25 in. length) sinker nails attached tie-down anchors to the end studs, and 13 gage x

1-1/2 in. drywall nails attached gypsum wallboard to the frame. A nail spacing of 6 in. perimeter and 12 in. field was used for the plywood sheathing and 7 in. perimeter and 10 in. field for the gypsum wallboard. Tie-down anchors were attached to the double end studs using the 16d sinker nails, one located in each of the 32 pre-punched holes in the metal anchor.

Table 3: Fastener schedule

Connection Description	No. and Type of Connector	Connector Spacing
Framing		
Top Plate to Top Plate (Face-nailed)	16d common	per foot
Top / Bottom Plate to Stud (End-nailed)	2-16d common	per stud
Stud to Stud (Face-nailed)	2-16d common	24 in. o.c.
Stud to Header (Toe-nailed)	2-16d common	per stud
Header to Header (Face-nailed)	16d common	16 in. o.c. along edges
Tie-down Anchor/ Anchor Bolts		
Tie-down Anchor to Stud (Face-nailed)	32-16d sinker	per tie-down
Tie-down Anchor to Foundation	1-A307 5/8 in. dia. bolt	per tie-down
Anchor bolts	1-A307 5/8 in. dia. bolt	24 in. o.c. and within 1 ft. of wall ends, using 3 x 3 x ¼ in. steel plate washers
Sheathing:		
Plywood	8d	6 in. edge / 12 in. field (2 rows for end stud)
Gypsum wall board	13 ga x 1½ in. (3/8 in. head)	7 in. edge / 10 in. field

<u>Wall Orientation and Attachment to Test Frame</u>

Tests were performed with the shear walls in a horizontal position as shown in Figures 2 - 3. The wall was raised approximately 16 inches above the ground to allow sufficient clearance for instruments and the load cell to be attached to the wall. The bottom plate was secured to a fixed steel structural tube at 24 in. on center. Oversize of bolt holes was limited to 1/32 in. to minimize slip.

Bolts attaching the bottom plate were located a minimum of 12 inches away from the studs adjacent to openings or end of wall. This resulted in the bottom plate lifting when the stud next to an opening was in tension. In turn, the nails attaching the sheathing

to the bottom plate had to transfer this tension at large displacements and were damaged significantly more than nails near tie-down anchors.
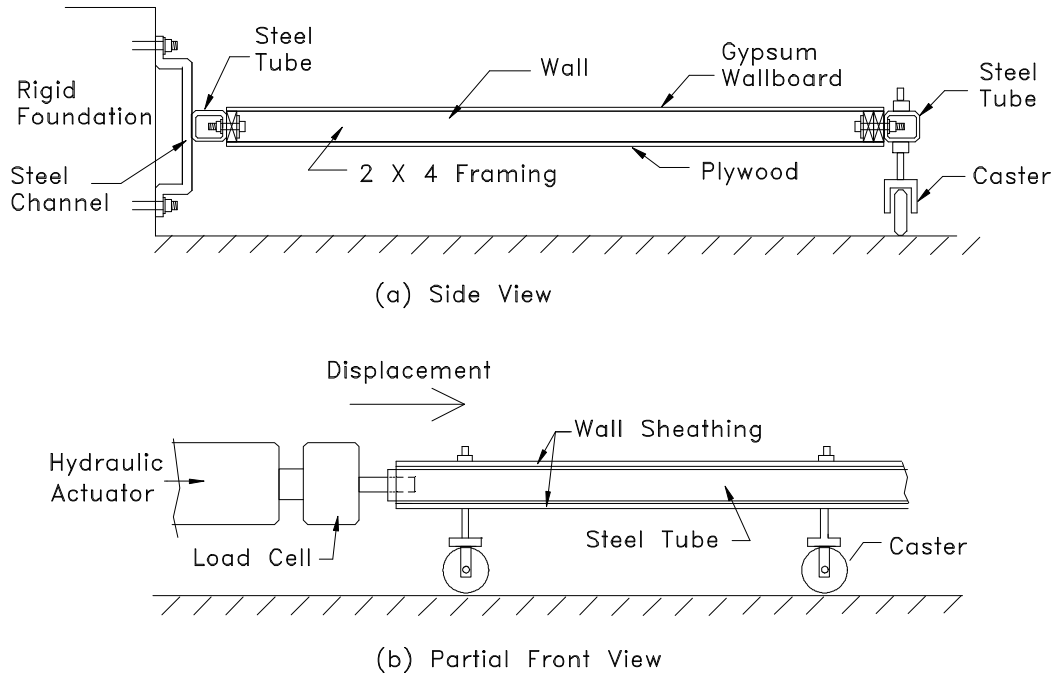

(a) Side View

(b) Partial Front View
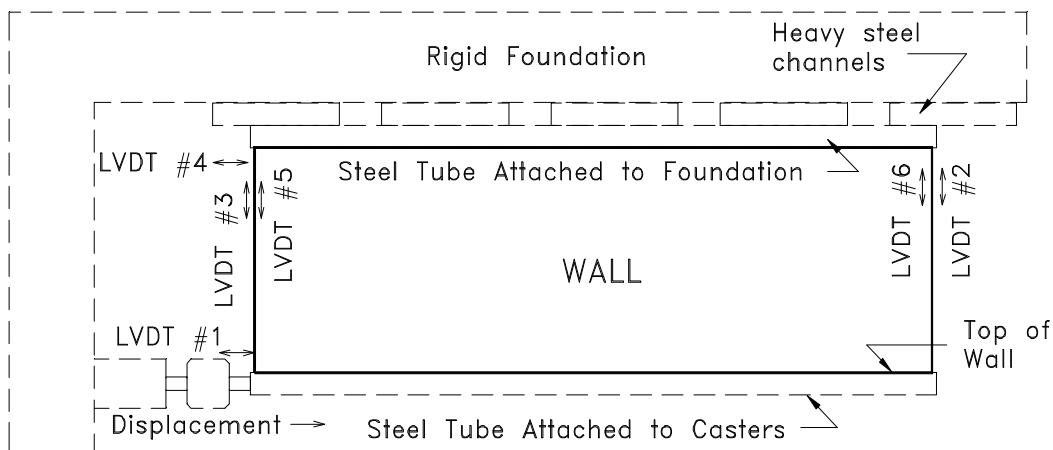
Figure 2: Wall orientation

Figure 3: Sensor locations on plan view of wall specimen

Test Equipment and Instrumentation

A hydraulic actuator, with a range of ±6 inches and capacity of 55,000 lbs, was attached to the top left corner of each shear wall (for the configurations shown in Table 1)

via a steel tube that was used to distribute the loading to the wall double top plate. The steel tube and the double top plate were attached using 5/8 in. diameter bolts 24 in. on center, beginning one foot from the end of the wall. Eight casters were attached to the structural tube to allow horizontal motion, as shown in Figure 2(b). The casters were fixed parallel to loading. A test was conducted to determine the amount of friction created by the wheels. Even though the magnitude of the friction was negligible (0.5 - 2%) when compared to the capacity of the walls, all recorded loads were corrected for this bias.

Figure 3 shows the location of the six LVDT's that were attached to the frame of each wall to measure wall displacements.

LVDT #1 was located adjacent to where the load was applied, measuring the displacement of the top of the wall relative to a fixed reference point.

LVDT #2 and LVDT #3 measured the compression and uplift displacement of the end studs relative to the foundation. These sensors determined the amount of crushing in the sill plate, or uplift of the end stud, depending on which corner of the wall was in compression or tension, respectively. All data recorded was corrected to compensate for amplifications caused by the geometry of the LVDT fixtures. This ensured the actual compression and uplift displacements of the end studs were measured.

LVDT #4 measured horizontal displacement of the bottom plate relative to a fixed point. This measurement allows rigid body translation of the wall to be subtracted from the global displacement to obtain interstory drift. Interstory drift is calculated as LVDT #1 - LVDT #4.

LVDT #5 and LVDT #6 were attached to the end studs and tie-down anchors. These sensors measured the slip, if any, of the tie-down anchors relative to the end stud.

The hydraulic actuator contained two internal sensors recording load resisted by the wall and relative displacement of the load cell.

The data acquisition system recorded data 50 times per second.

Loading

The method used to test the walls in this study was a modification of the "Sequential Phased Displacement" procedure used by the Joint Technical Coordinating Committee on Masonry Research (TCCMAR) for the United States-Japan Coordinated Earthquake Research Program. Sequential phased displacement (SPD) loading consisted of two displacement patterns and is illustrated in Figure 4. The first pattern gradually displaced the wall to its anticipated yield displacement. Elastic behavior of the wall was observed in this section of the test. The second displacement pattern began once the wall had past its anticipated yield displacement (i.e. inelastic behavior) or first major event (FME). The FME used in these tests was determined from monotonic test results. Figure 5 displays one phase of SPD loading after the anticipated yield displacement had been reached. The displacement was a triangular, sinusoidal ramp function at a frequency of 0.5 Hz.

The first displacement pattern consisted of reversed-cyclic displacements for three cycles at each incremental level at low, elastic behavior displacement levels. The first set of three cycles displaced the wall at approximately 25% of the FME. The second set of three cycles displaced the wall 50% of the FME and the final set of three cycles displaced

the wall at 75% of the FME. The next cycle displaced the wall to approximately the FME. At this point, the wall started to behave in an inelastic manner and the second displacement pattern began.
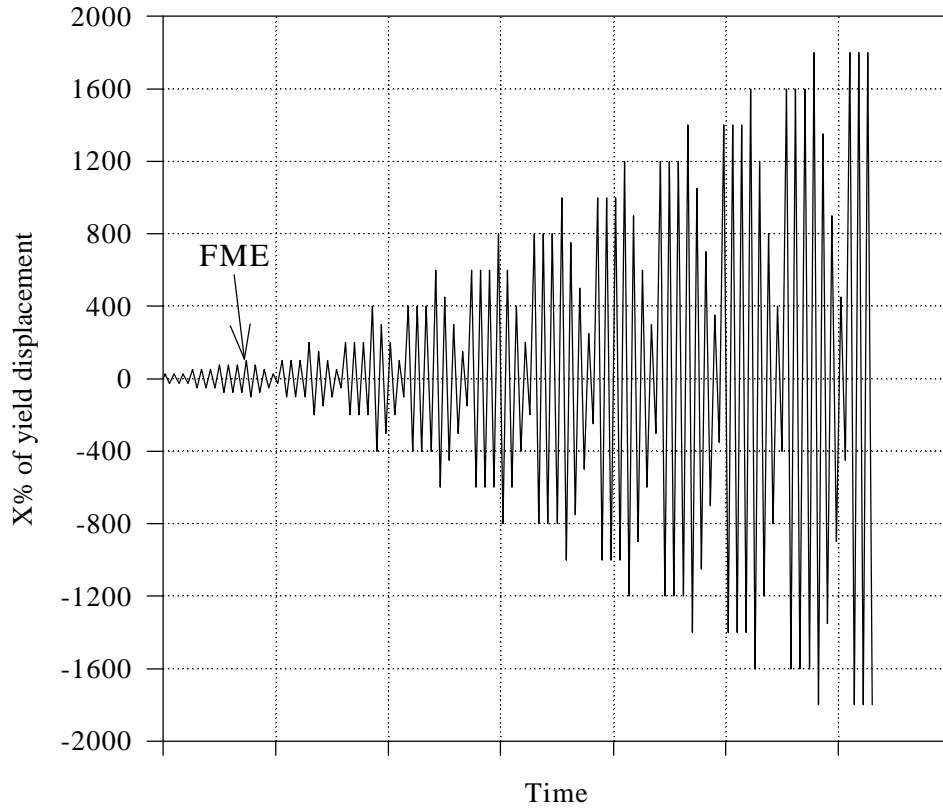

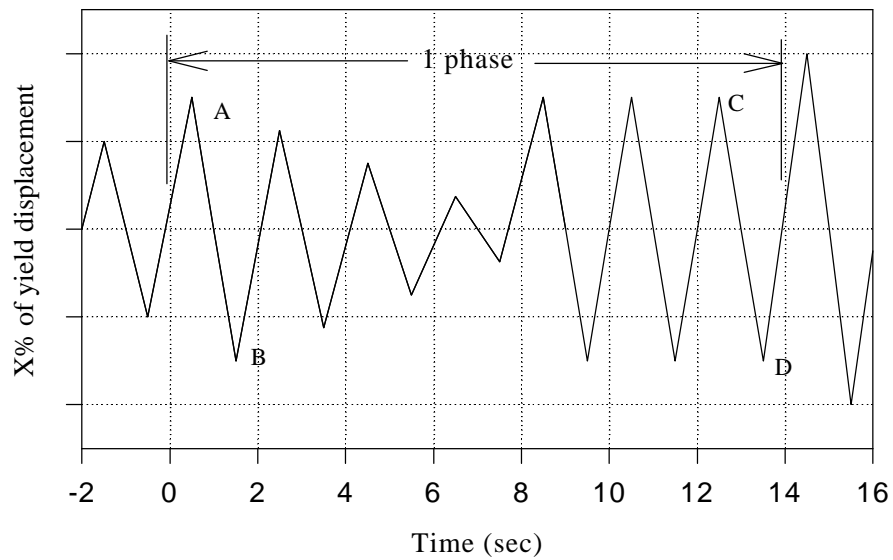**Figure 4: Displacement pattern used in sequential phased displacement**

Figure 5: Single phase of sequential phased displacement pattern

For the first two cyclic tests with Wall A and Wall D, a FME of 1.0" was used. It was observed that the gypsum board failed before the anticipated yield FME displacement under cyclic loading. For this reason, the FME was changed to 0.1" for the remaining tests of Wall B, Wall C and Wall E. Wall A was repeated with an FME of 0.1" with minimal reduction in initial and stabilized resistance, indicating that data from Wall A and Wall D with a FME of 1.0"could be compared with tests with a FME of 0.1".

Figure 5 graphically illustrates one phase of the second displacement pattern in SPD loading. Once yielding occurred, the displacement of each set of cycles was based on the previous set of cycles. Peak displacement of a set of cycles was increased 200% of the FME displacement over the previous set of cycles. The first peak cycle of a set was followed by three decay cycles, with each magnitude 25% less than the previous cycle (i.e. the first decay cycle was 75% of the peak displacement, second was 50%, and third was 25%). Following the decay cycles were three cycles at the peak displacement. Three cycles were determined to be sufficient in order to obtain a "stabilized" response for nailed shear walls. "Stabilized" response was defined as when the load resisted by the wall, when displaced the same magnitude in two successive cycles, did not decrease more than 5%.

PROPERTY DEFINITIONS

All properties determined in this investigation were based on initial and stabilized cyclic response.

Initial and stabilized load envelope curves, similar to the ones shown in Figure 6, were determined for each wall. The initial load envelope curve consists of positive and negative peak loads and corresponding displacements of the first cycle (corresponding to points A and B in Figure 5) in each phase of SPD loading. The stabilized load envelope curve consists of positive and negative peak loads and corresponding displacements in the last cycle of each phase (corresponding to points C and D in Figure 5.) The hysteresis and construction of the initial and stabilized load envelope curves is illustrated for each wall specimen in Appendix A.

The average of the peak positive and negative load resisted in the first cycle of a given phase was taken as the initial cycle load resisted at the corresponding interstory drift. The highest average load resistance occurring in the first cycle was taken as the initial capacity, $F_{max,init}$. Similarly, the highest average load resistance occurring in the last cycle was taken as the stabilized capacity, $F_{max,stab}$. Interstory drifts corresponding to initial and stabilized capacity were determined and denoted as $\Delta_{max,init}$ and $\Delta_{max,stab}$, respectively.

Failure of the walls was defined as a significant drop in load resistance. Drift at failure is designated as $\Delta_{failure}$ and is necessary for computing ductility.

Elastic stiffness, k_e, was defined as the slope of the line passing through the origin and the point on the load envelope curve where the load equals 40% of F_{max}. This stiffness represents a good estimate of the stiffness that shear walls will exhibit after being loaded a number of times at low to moderate magnitudes.
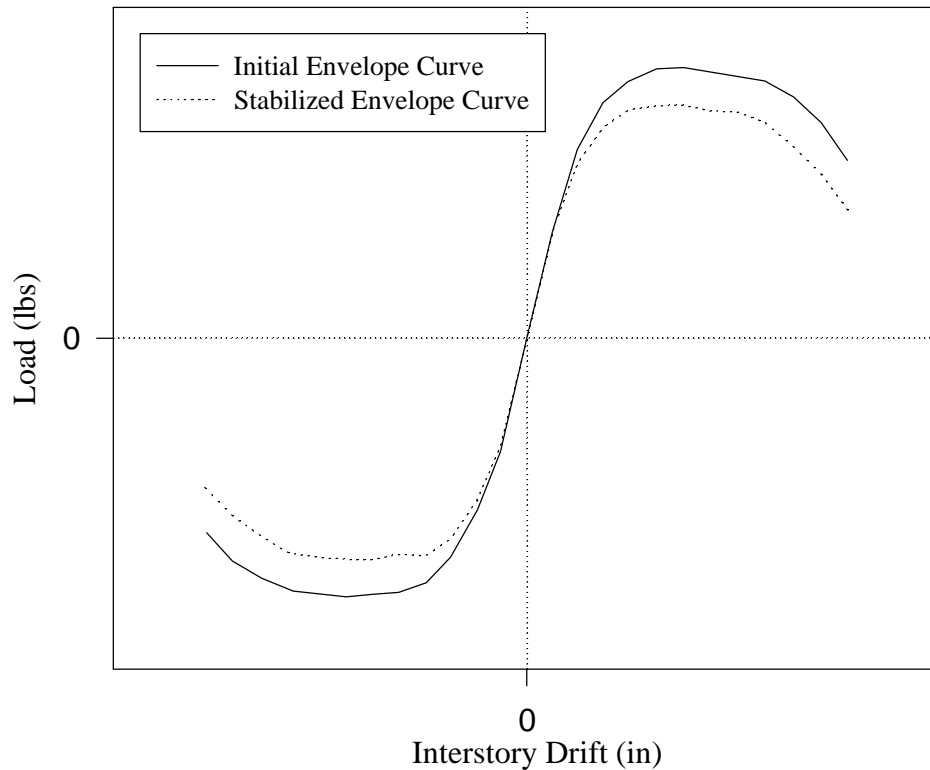
Figure 6: Typical initial and stabilized load envelope curves

An equivalent energy elastic-plastic curve, used for comparison purposes, was determined for each wall. This artificial curve, shown in Figure 7, depicts how an ideal perfectly elastic-plastic wall would perform and dissipate an equivalent amount of energy. The equivalent elastic-plastic curve (EEPC) was defined so that the area under the EEPC is equal to the area under the load-displacement curve from 0" drift to $\Delta_{failure}$. The elastic portion of the EEPC contains the origin and has a slope equal to the elastic stiffness, k_e. The plastic portion of the EEPC is a horizontal line positioned so that the EEPC and load-displacement curve areas are equal (i.e. areas A1 and A2 in Figure 7 are equal). Displacement at yield, Δ_{yield}, and load at yield, F_{yield}, were defined as the intersection of the elastic and plastic lines of the EEPC. F_{yield} must be greater than or equal to 80% of F_{max}. This definition of the EEPC was also used in the monotonic tests.

Ductility is determined from the equivalent elastic-plastic curve and is defined as:

$$D = \frac{\Delta_{failure}}{\Delta_{yield}}$$

(5)

where D is the ductility, and $\Delta_{failure}$ and Δ_{yield} are defined in Figure 7. $\Delta_{failure}$ was defined as the deflection where a significant drop in load resistance was observed.

It should be noted that alternative definitions have been proposed by organizations such as the Structural Engineers Association of Southern California, and some proposals do not promote the use of ductility ratio. However, it is an indication of how structural

systems fail (brittle or ductile), and is therefore a useful parameter to be considered when determining how to convert test results to design values.
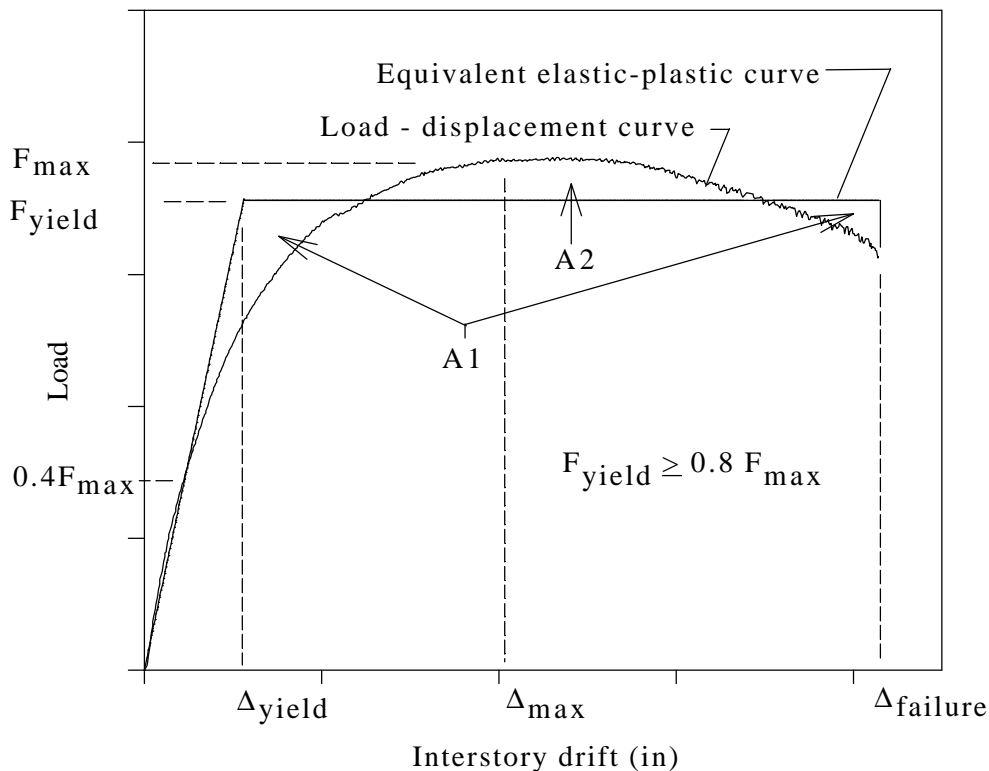

Figure 7: Typical equivalent-energy, elastic-plastic load-displacement curve

SPD TEST RESULTS

Strength

Load resistance at capacity, and at interstory drifts of 0.32", 0.96" and 1.6" was determined from the initial and stabilized load envelope curves and is presented in Table 4. Table 5 presents information on the equivalent elastic-plastic curve parameters. The envelope curves for each specimen are illustrated in Appendix A.

Initial cyclic capacity ranged from 7.5 kips for Wall E to 32.0 kips for Wall A, and stabilized cyclic capacity ranged from 6.6 kips for Wall E to 27.5 kips for Wall A. As expected, capacity increased as sheathing area ratio of each wall increased.

The ratio of the stabilized load to initial cycle load is included in each section of Table 4. This ratio indicates the resistance decrease due to the repetitive cyclic load. At displacements near capacity, the reduction between the initial and stabilized resistance remains fairly constant with the stabilized resistance approximately 85 percent of the initial resistance. At low displacements the stabilized resistance is 90 percent of the initial cycle (with the exception of the fully sheathed wall.)

At an interstory drift of 1.6", initial cyclic load resistance ranged from 7.2 kips to 30.6 kips, and stabilized cyclic load resistance ranged from 6.4 kips to 26.5 kips. At 0.96" drift, initial cyclic load resistance ranged from 7.1 kips to 31.7 kips, and stabilized cyclic load resistance ranged from 6.3 kips to 27.1 kips. At 0.32" drift, initial cyclic load resistance ranged from 4.6 kips to 30.6 kips, and stabilized cyclic load resistance ranged from 4.2 kips to 26.5 kips. As expected, load resistance increased as sheathing area ratio of each wall increased.

Table 4: Initial cyclic and stabilized cyclic load resistance data

| | Wall Configuration | | | | |
	A	B	C	D	E
Capacity					
Initial (kips)	32.0	20.3	13.6	11.5	7.5
Stabilized (kips)	27.5	17.4	11.8	9.9	6.6
Stabilized / Initial	0.85	0.86	0.87	0.86	0.88
Load at 1.6"					
Initial (kips)	30.6	19.3	13.4	10.8	7.2
Stabilized (kips)	26.5	16.5	11.8	9.5	6.4
Stabilized / Initial	0.87	0.85	0.88	0.88	0.89
Load at 0.96"					
Initial (kips)	31.7	18.9	11.8	10.8	7.1
Stabilized (kips)	27.1	16.3	11.4	9.5	6.3
Stabilized / Initial	0.85	0.86	0.97	0.88	0.89
Load at 0.32"					
Initial (kips)	30.6	11.1	6.1	5.4	4.6
Stabilized (kips)	26.5	10.7	5.9	5.5	4.2
Stabilized / Initial	0.87	0.96	0.97	1.01	0.91

Yield Load

The equivalent energy yield loads for each wall configuration are shown in Table 5 along with the ratio of the yield load to the respective capacity. As expected, the yield load values follow the wall capacities with the fully sheathed wall having the highest capacity and the wall with the least sheathing having the lowest yield load. However, the ratio of the yield load to the respective capacity remains fairly constant, and the values fall in a narrow range between 0.88 and 0.93.

Stiffness

Elastic stiffness, taken as the secant slope at 40% of capacity for the respective curves, is presented in Table 5. The initial and stabilized stiffness values are essentially

equivalent which reinforces the impression that wood shear walls do not show significant damage at low displacements(i.e., less than 0.32 in.) Initial cyclic elastic stiffness ranged from 18.1 kips/in to 69.7 kips/in. Stabilized cyclic elastic stiffness ranged from 18.0 kips/in to 69.2 kips/in. In both cases the fully sheathed wall had the highest stiffness. It should be noted that the stiffness shown in Table 5 and the capacities shown in Table 4 follow the same trend (i.e. an increase in magnitude as area of openings decreases).

Table 5: Equivalent elastic-plastic curve parameters

	Wall Configuration				
	A	B	C	D	E
F_{yield}					
Initial (kips/in)	29.9	18.2	12.2	10.5	6.7
Stabilized (kips/in)	25.7	15.6	10.7	9.1	5.8
Initial: Yield / Capacity	0.93	0.90	0.90	0.91	0.89
Stabilized: Yield / Capacity	0.93	0.90	0.91	0.92	0.88
Elastic Stiffness					
Initial (kips/in)	69.7	40.0	19.9	18.1	18.2
Stabilized (kips/in)	69.2	41.8	20.3	18.2	18.0
Ductility:					
Initial ductility	4.5	4.3	3.5	3.3	5.3
Δ_{yield} (in)	0.43	0.47	0.62	0.58	0.37
$\Delta_{failure}$ (in)	1.93	2.00	2.19	1.94	1.97
Stabilized ductility	5.2	5.2	4.1	4.0	6.2
Δ_{yield} (in)	0.37	0.38	0.53	0.49	0.32
$\Delta_{failure}$ (in)	1.93	1.98	2.17	1.95	1.98
Stabilized/ Initial ductility	1.15	1.20	1.18	1.20	1.18

Ductility

Equation (5) was used to determine the ductility ratio from the initial and stabilized equivalent elastic-plastic curves. As presented in Table 5, initial cycle ductility ranged from 3.3 to 5.3, and stabilized cycle ductility ranged from 4.0 to 6.2. The ratio of stabilized to initial ductility ranged from 1.15 to 1.20.

End Stud Movement

Movement of the end studs relative to the bottom plate was observed. The distance traveled by the end studs between peak positive and negative interstory drifts (i.e.

between point A to B in Figure 4), recorded during the initial cycle at Δ_{max} and $\Delta_{failure}$, are given in Table 6. The reported movement of the end studs was determined at 1.5" from the end of the wall (i.e. the center of the double end studs) near the bottom plate.

Left end stud movement at Δ_{max} ranged from 0.10" to 0.18" and right end stud movement at Δ_{max} ranged from 0.10" to 0.14". The hold-down anchors are responsible for keeping movement of the end studs to a minimum. At failure, left end movement ranged from 0.19" to 0.21" and right end stud movement ranged from 0.14" to 0.23". Measured displacement is primarily due to rotation of the bottom of the end stud about the tie-down anchor bolts and wood crushing.

Table 6: End stud displacement between positive and negative peak drifts during initial cycle of Δ_{max} and $\Delta_{failure}$

	Wall Configuration				
	A	B	C	D	E
Left end stud (LVDT #1) at Δ_{max}	0.14"	0.12"	0.18"	0.10"	0.10"
Right end stud (LVDT #2) at Δ_{max}	0.14"	0.10"	0.10"	0.14"	0.14"
Left end stud (LVDT#1) at $\Delta_{failure}$	0.21"	0.19"	0.21"	*	0.20"
Right end stud (LVDT #2) at $\Delta_{failure}$	0.20"	0.17"	0.14"	0.20"	0.23"

* sensors did not record data

Tie-down Anchors

For purposes of monitoring slip between the anchor and the end stud, a LVDT was placed on each metal tie-down anchor during loading. The slip relative to the stud for anchors, recorded near maximum load, was found to be negligible for all wall configurations tested using cyclic loading.

Gypsum Wallboard

Gypsum panels were observed to perform poorly during the cyclic tests. Even at low displacement magnitudes, drywall nails tore a path in the gypsum panels. Failure of taped joints failed at lower interstory drifts than during monotonic tests. Similar to monotonic tests, gypsum board panels underwent rigid body motion about their centers.

Plywood Sheathing

Similar to the monotonic tests, full height plywood panels performed in a racking manner while plywood sheathing above openings did not rack. Panels below openings experienced some racking. Predominant failure of the plywood sheathing was due to failure of the nails. Nails experienced partial withdrawal from the framing and fatigue. Nailing on the perimeter of panels, especially near corners, experienced more fatigue than field nailing. Some tear through the edge of plywood panels was observed, but the

amount was significantly less than in monotonic tests. The predominant mode of failure was fatigue of the plywood nailing.

General Observations

Failure modes for walls with openings had many similarities. Typical failures occurred when all of the sheathing nails at the bottom or top plate for one of the wall segments failed. This lead to a progression of failures of the remaining wall segments. Interior wall segments were always the first to fail due to the absence of tie-down restraint. Wall A, the fully sheathed wall did not show the complete failure of the nails at the bottom or top of the wall, and survived the complete SPD displacement regime.

These tests were performed without an applied dead load in order to test the most conservative condition. If dead load had been present, the studs next to the openings that had no overturning restraint (i.e., no tie-down connectors) would not have lifted from the test frame as much. This would have reduced the damage to the nails attaching the sheathing to the bottom plate in these regions. The result would have been an improved overall performance. This is especially clear when one considers that studs next to openings have the highest axial load due to applied dead load.

Comparison to Monotonic Performance

The monotonic and cyclic capacity (maximum loads) are compared in Table 7. The monotonic and cyclic yield loads, F_{yield}, elastic stiffness values, ductilities, displacements at yield, Δ_{yield}, and displacement at failure, $\Delta_{failure}$, are compared in Table 8. In all cases, the basis of comparison is the monotonic values.

The initial cyclic capacity for the walls ranged from 82 to 99 percent of the monotonic capacity for the walls, with the fully sheathed wall having the largest reduction and Wall C (r = 0.55) having the lowest reduction in capacity. The stabilized maximum load ranged between 71 and 86 percent of the monotonic capacity, with the fully sheathed wall having the largest reduction and Wall C having the lowest reduction.

Table 7: Monotonic and Cyclic Capacities.

	Wall Configuration				
	A	B	C	D	E
Capacity: (kips)					
Monotonic	38.8	23.1	13.8	12.1	8.2
Initial Cyclic	32.0	20.3	13.6	11.5	7.5
Stabilized Cyclic	27.5	17.4	11.8	9.9	6.6
Initial / Monotonic	0.82	0.88	0.99	0.95	0.91
Stabilized / Monotonic	0.71	0.75	0.86	0.82	0.80

Table 8: Monotonic and Cyclic Yield Loads Elastic Stiffness, Ductility, and Yield and Failure Displacements.

| | Wall Configuration | | | | |
	A	B	C	D	E
Yield Load: (kips)					
Monotonic	35.6	20.9	11.8	10.6	7.5
Initial Cyclic	29.9	18.2	12.2	10.5	6.7
Stabilized Cyclic	25.7	15.6	10.7	9.1	5.8
Initial / Monotonic	0.84	0.87	1.03	0.99	0.89
Stabilized / Monotonic	0.72	0.75	0.91	0.86	0.77
Elastic Stiffness: (kips/in)					
Monotonic	63.7	43.7	22.2	19.4	7.8
Initial Cyclic	69.7	40.0	19.1	18.1	18.2
Stabilized Cyclic	69.2	41.8	20.3	18.2	18.0
Initial / Monotonic	1.09	0.92	0.86	0.93	2.33
Stabilized / Monotonic	1.09	0.96	0.91	0.94	2.31
Ductility:					
Monotonic	7.4	8.7	7.3	8.8	5.2
Initial Cyclic	4.5	4.3	3.5	3.3	5.3
Stabilized Cyclic	5.2	5.2	4.1	4.0	6.2
Initial / Monotonic	0.61	0.49	0.48	0.38	1.02
Stabilized / Monotonic	0.70	0.60	0.56	0.45	1.19
Yield Displacement: (in)					
Monotonic	0.56	0.48	0.55	0.57	0.98
Initial Cyclic	0.43	0.47	0.62	0.58	0.37
Stabilized Cyclic	0.37	0.38	0.53	0.49	0.32
Initial / Monotonic	0.77	0.98	1.13	1.01	0.38
Stabilized / Monotonic	0.66	0.79	0.96	0.86	0.33
Failure Displacement: (in)					
Monotonic	4.14	4.18	4.00	5.04	5.05
Initial Cyclic	1.93	2.00	2.19	1.94	1.97
Stabilized Cyclic	1.93	1.98	2.17	1.95	1.98
Initial / Monotonic	0.47	0.48	0.55	0.38	0.39
Stabilized / Monotonic	0.47	0.47	0.54	0.39	0.39

Yield load followed the same trend, with the initial cycle yield load being between 84 and 103 percent of the respective value for the monotonic test. Stabilized yield load was between 72 and 91 percent of the respective value for the monotonic test.

Elastic stiffness for the initial cycle response ranged from 86 to 93 percent of the monotonic value for Walls B, C, and D. Stabilized elastic stiffness for the same walls ranged from 91 to 96 percent of the monotonic elastic stiffness. The fully sheathed wall (Wall A) and wall with the lowest sheathing area ratio (Wall E) increased in stiffness when tested under cyclic loading, 9 and 133 percent respectively. The significant increase in stiffness associated with Wall E may be due to a combination of the effect of the tie-down anchors, the definition of stiffness, and the inherent variability of wall performance. Wall E had tie-down anchors attached to each of the two wall segments with a single sheet of sheathing attached to each segment. Walls with interior wall segments, which did not have tie-down restraint, had reduced elastic stiffness when subjected to cyclic loading due to the damage experienced at the top and bottom of the wall segments. The definition of elastic stiffness has a significant effect, in that the elastic stiffness line is plotted from the origin through the point on the load-displacement curve with a resistance of 0.4 F_{max} . This results in the stiffness being indirectly affected by the capacity

With the exception of Wall E, the ductility was reduced more for walls with smaller sheathing area ratios when subjected to cyclic loading. This is shown by the ratios of initial to monotonic and stabilized to monotonic values. Wall A has the least reduction, while wall D has the highest reduction. Wall E actually increased slightly in ductility. The increase may be due to the fact that both of the wall segments for Wall E had one tie-down connection, and therefore would not experience as much cyclic damage as would wall segments without tie-down connections.

Yield displacement values showed no significant trends other than that the stabilized yield displacement was always smaller than the monotonic value.

Failure displacement for the walls tested with cyclic displacements was always less than half of the monotonic value. The exception was Wall C, which had a cyclic value slightly higher than half of the monotonic value. This is expected since the SPD test subjects the nails used to attach the sheathing to the framing to a high number of cycles. This results in fatigue damage to the nails and a failure at lower displacements. It should be noted that nail fatigue is not a typical failure mode for wind and seismic loading. However, the SDP test results should provide conservative design and analytical values for these types of repetitive cyclic loading.

Application of Equation (1)

Shear capacity ratios, as defined in TE-1996-001 and Equation (1), were determined for the initial and stabilized curves at capacity. Actual shear capacity ratio at capacity was determined as the maximum load resisted by a shear wall with openings divided by the maximum load resisted by a shear wall of the same dimensions without openings. Equation (1) was developed based shear walls loaded monotonically, and results of cyclic tests of shear walls were not available. Therefore, it was not possible to verify if shear capacity ratios determined in Equation (1) were valid for cyclic loading.

At capacity, Equation (1) was used for predicting shear capacity ratios. Table 9 and Figure 8 show actual shear capacity ratios from the initial and stabilized curves for

cyclic tests, along with prediction made from Equation (1). As shown in Figure 8, the actual shear capacity ratio was higher than the predicted for all cases. This indicates that the wall specimens were stronger than predicted, and Equation (1) conservatively predicts cyclic capacity when the cyclic capacity for a fully sheathed wall is used as the base capacity. As shown in TE-1996-001, Equation (1) also conservatively predicts monotonic capacity when the monotonic capacity for a fully sheathed wall is used as the base capacity. The reserve capacity of walls tested cyclically, as indicated by the ratio of actual/ predicted shear capacity ratio, being greater than 1.0, is 24 - 85% for walls with openings. As can be seen by the actual/predicted shear capacity ratio, Equation (1) provides a more conservative design value for cyclic response as the sheathing area ratio decreases (i.e. the amount of openings increases). Equation (1) is more conservative for cyclic loads (24 - 85%) than for monotonic loads (17 - 68%).

Table 9: Application of Perforated Shear Wall Method to cyclic tests

	Wall Configuration				
	A	B	C	D	E
Predicted Shear capacity ratio (F)	1.0	0.51	0.29	0.24	0.13
Initial Cycle					
Capacity (kips)	32.0	20.3	13.6	11.5	7.5
Actual Shear capacity ratio (F)	1.0	0.63	0.43	0.36	0.23
(F) Actual/ (F) Predicted	1.0	1.24	1.48	1.50	1.77
Stabilized Cycle					
Capacity (kips)	27.5	17.4	11.8	9.9	6.6
Actual Shear capacity ratio (F)	1.0	0.63	0.43	0.36	0.24
(F) Actual / (F) Predicted	1.0	1.24	1.48	1.50	1.85
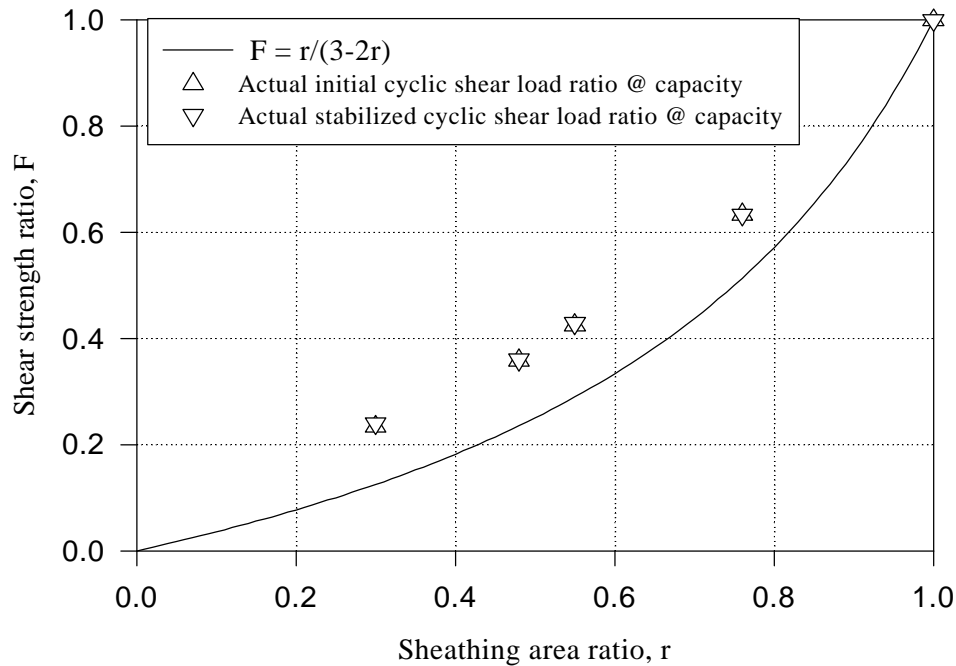
Figure 8: Initial and stabilized shear capacity ratios at capacity

Conclusions

Information concerning the behavior of full-scale tests of shear walls experiencing cyclic loading has been presented. This information includes quantification of the initial and stabilized capacity, elastic stiffness and ductility. Slip of the tie-down anchors was not a factor in failure of any of the walls tested. Tie-down anchors prevented excessive movement of the end studs relative to the bottom plate.

Comparisons between cyclic and monotonic performance were made which quantify the differences in resistance, stiffness, ductility, and other performance variables.

It was shown that the perforated shear wall method for wood shear walls provides conservative estimates of cyclic capacity when the cyclic capacity of fully sheathed walls is used as the basis. The conservatism increases as the amount of openings increases.

References

American Forest & Paper Association (AF&PA), 1995, Wood Frame Construction
        Manual for One- and Two- Family Dwellings - SBC High Wind Edition. American
        Forest & Paper Association, Washington, D.C.

Dolan, J.D. and A.C. Johnson, 1996. *Monotonic Tests of Long Shear Walls with
        Openings*. Virginia Polytechnic Institute and State University Timber
        Engineering Report TE-1996-001.

Johnson, A.C., 1997. *Monotonic and Cyclic Performance of Full-Scale Timber Shear
        Walls with Openings*, thesis submitted in partial fulfillment of Master's of Science
        Degree in Civil Engineering. Virginia Polytechnic Institute and State University,
        Blacksburg, Virginia.

Porter, M.L., 1987. "Sequential Phased Displacement (SPD) Procedure for TCCMAR
        Testing." Proceedings of the Third Meeting of the Joint Technical Coordinating
        Committee on Masonry Research, U.S. - Japan Coordinated Earthquake Research
        Program, Tomamu, Japan.

Standard Building Code, 1994 with 1996 Revisions, Southern Building Code Congress
International,   Burmingham, AL.

Sugiyama, H. and Matsumoto, T., 1993. "A Simplified Method of Calculating the Shear
        Strength of a Plywood-Sheathed Wall With Openings II. Analysis of the Shear
        Resistance and Deformation of a Shear Wall With Openings." *Mokuzai Gakkaishi*,
        39(8):924-929.

Sugiyiama, H. and Matsumoto, T., 1994. "Empirical Equations for the Estimation of
        Racking Strength of a Plywood-Sheathed Shear Wall with Openings." Summaries
        of Technical Papers of Annual Meeting, *Trans. of A.I.J.*

<u>Appendix A</u>

This appendix contains load-deflection curves determined from the cyclic tests of Walls A - E, respectively. The curves are grouped into five groups and each group is organized in the same manner as follows:

The first figure of a group illustrates the entire load deflection history experienced by the walls during the SPD test.

The second figure illustrates hysteresis loops from the initial cycle for each phase of SPD loading until failure is reached.

The third figure illustrates hysteresis loops from the stabilized cycle for each phase of SPD loading until failure is reached.

The fourth figure illustrates initial and stabilized load envelope curves determined from the second and third figures for each group.
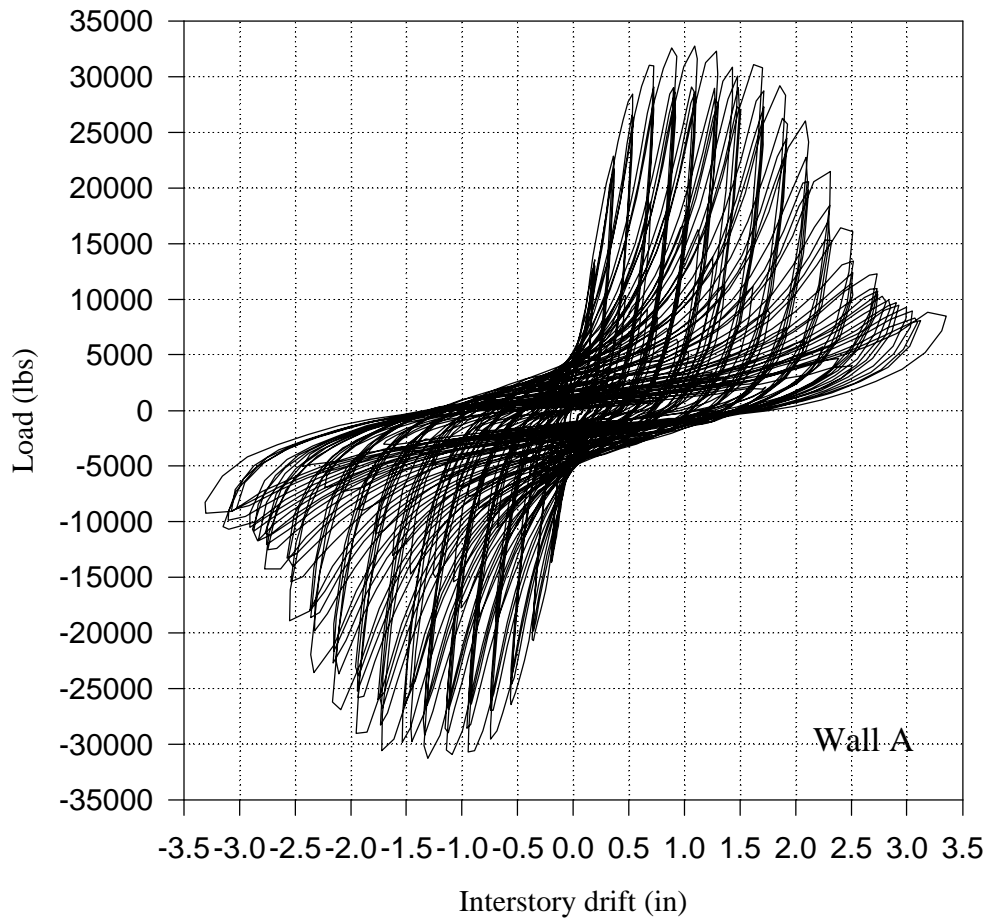
Figure A1-1: Load deflection history of Wall A (r = 1.0)
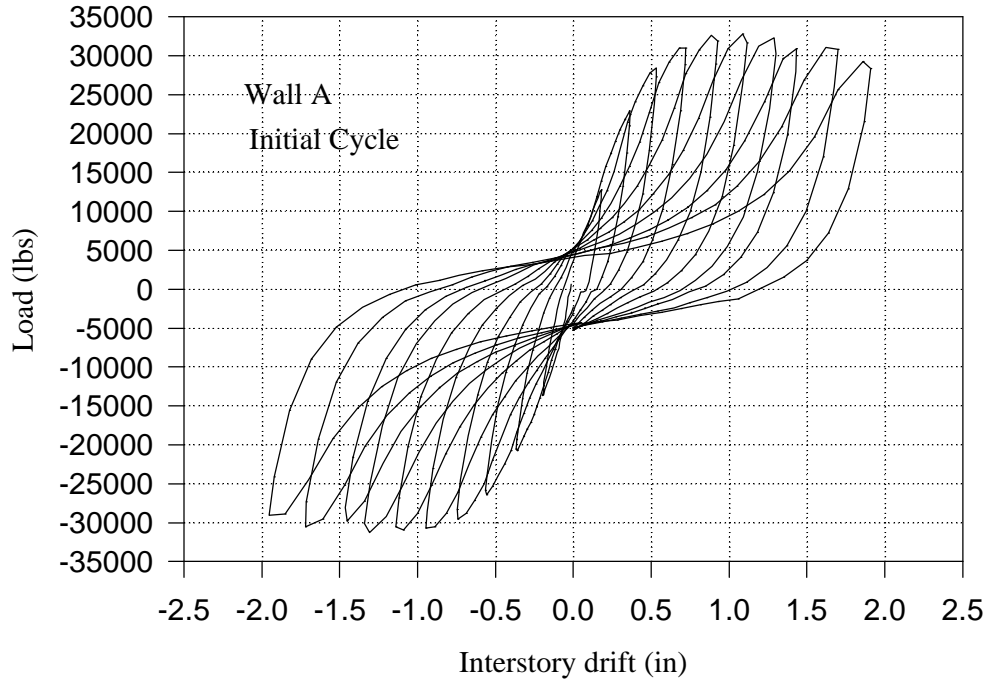
Figure A1- 2: Initial cycle hysteresis loops of Wall A
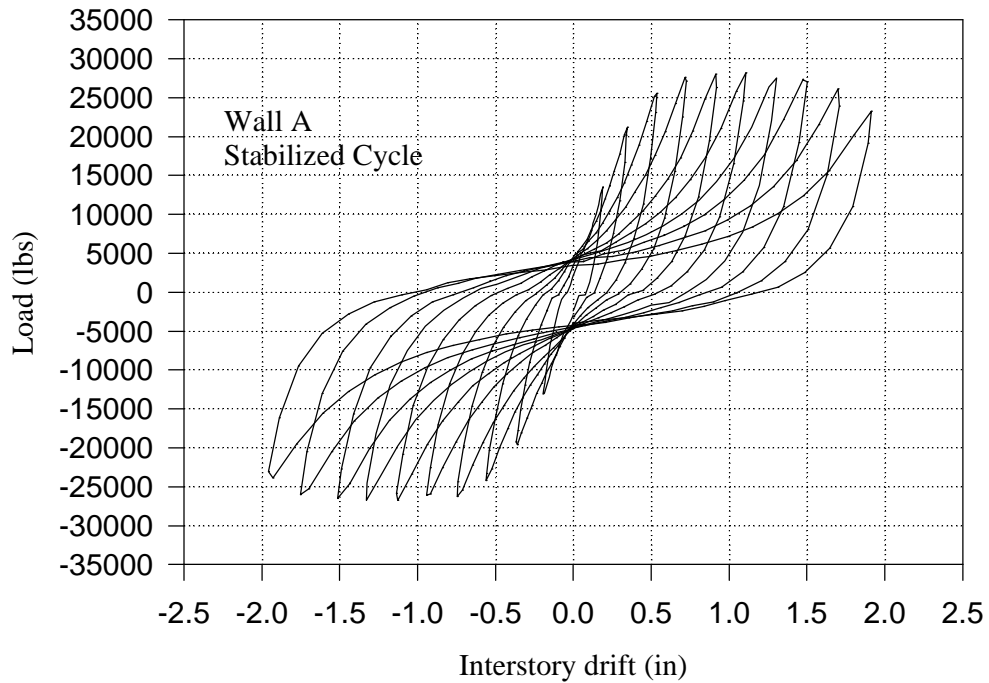
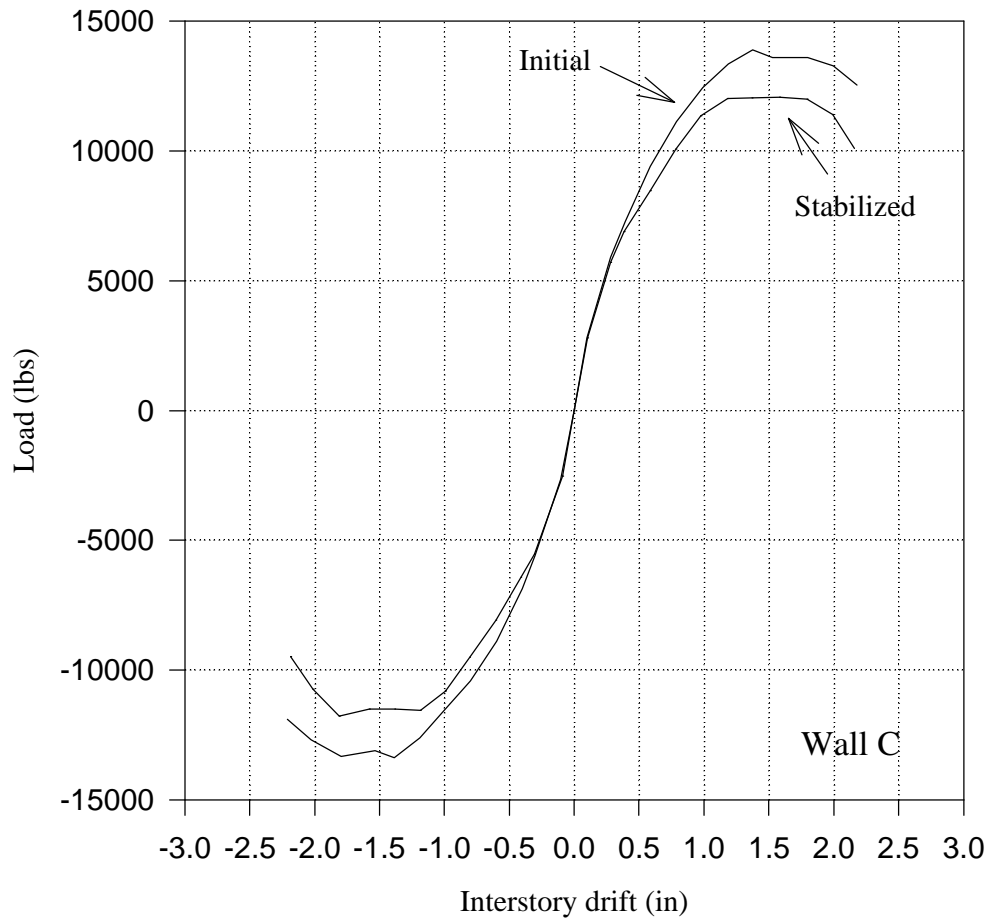**Figure A1- 3: Stabilized cycle hysteresis loops of Wall A**
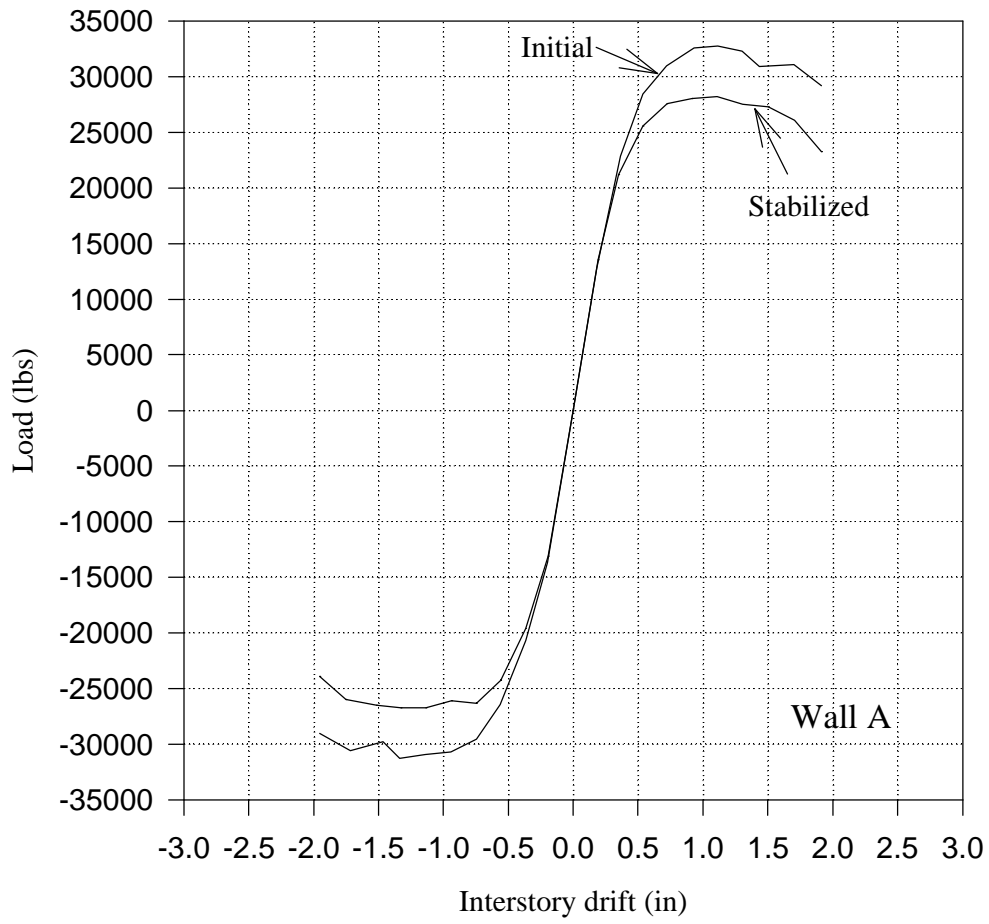
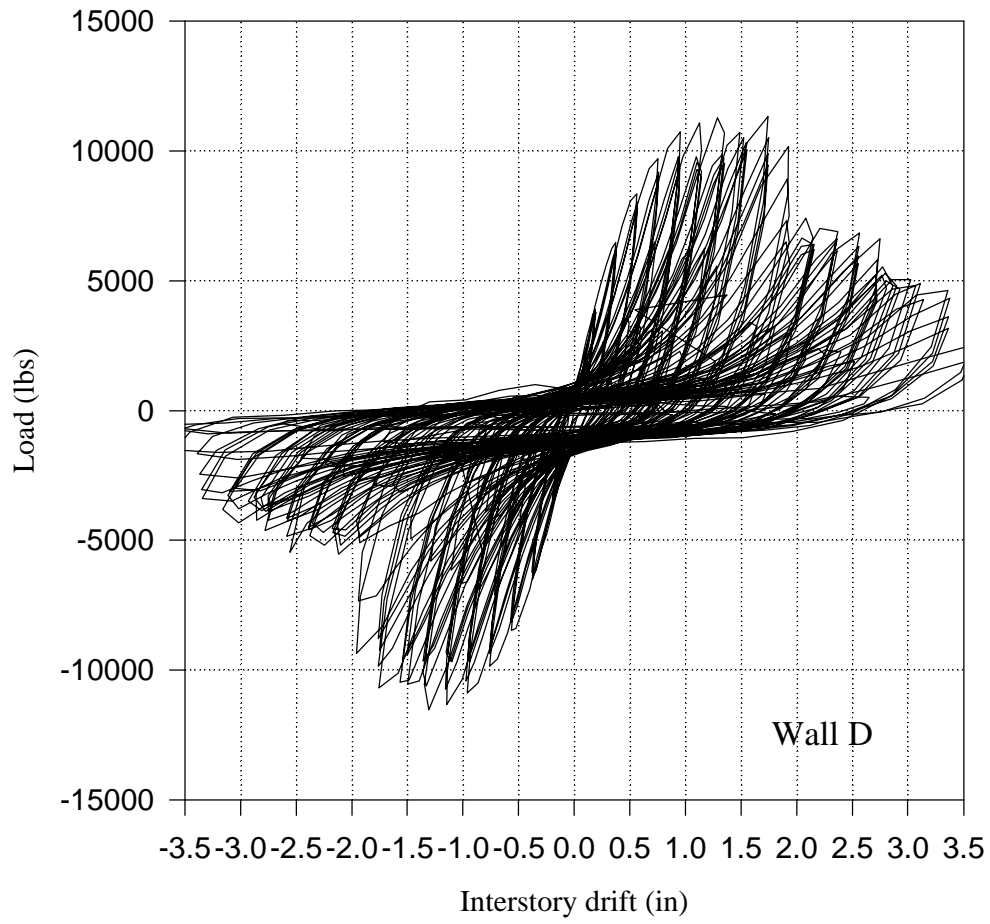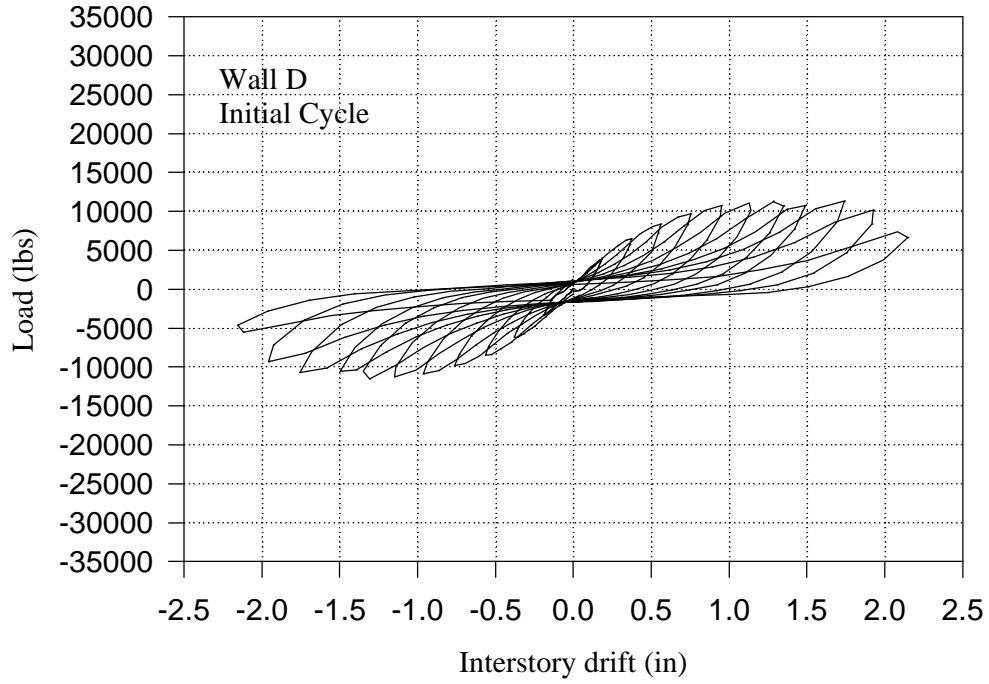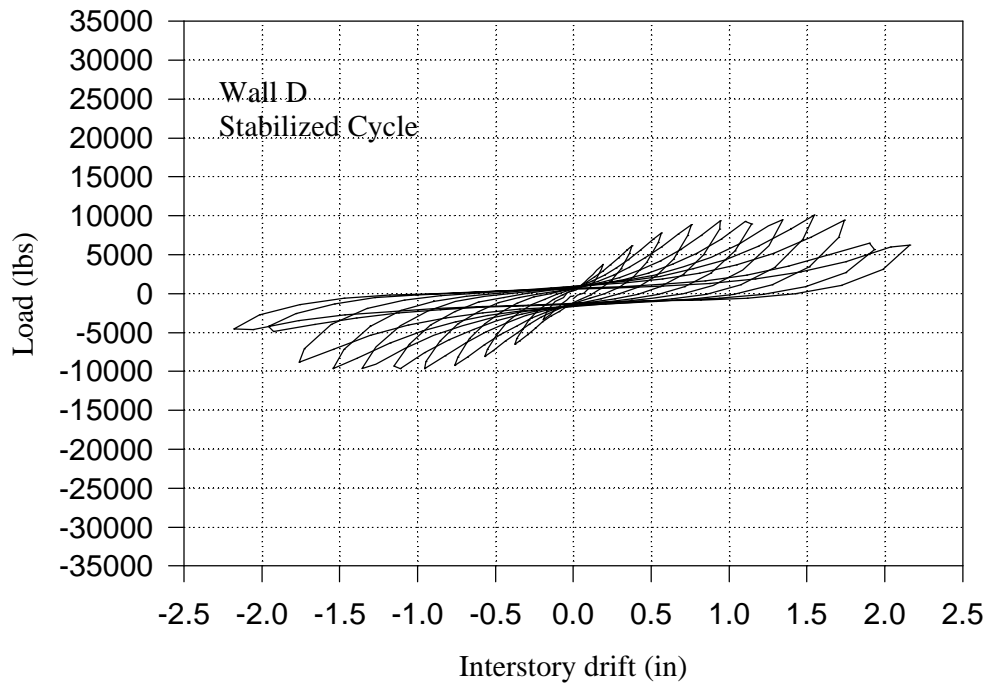**Figure A1-4: Initial and stabilized load envelope curves for Wall A (r = 1.0)**
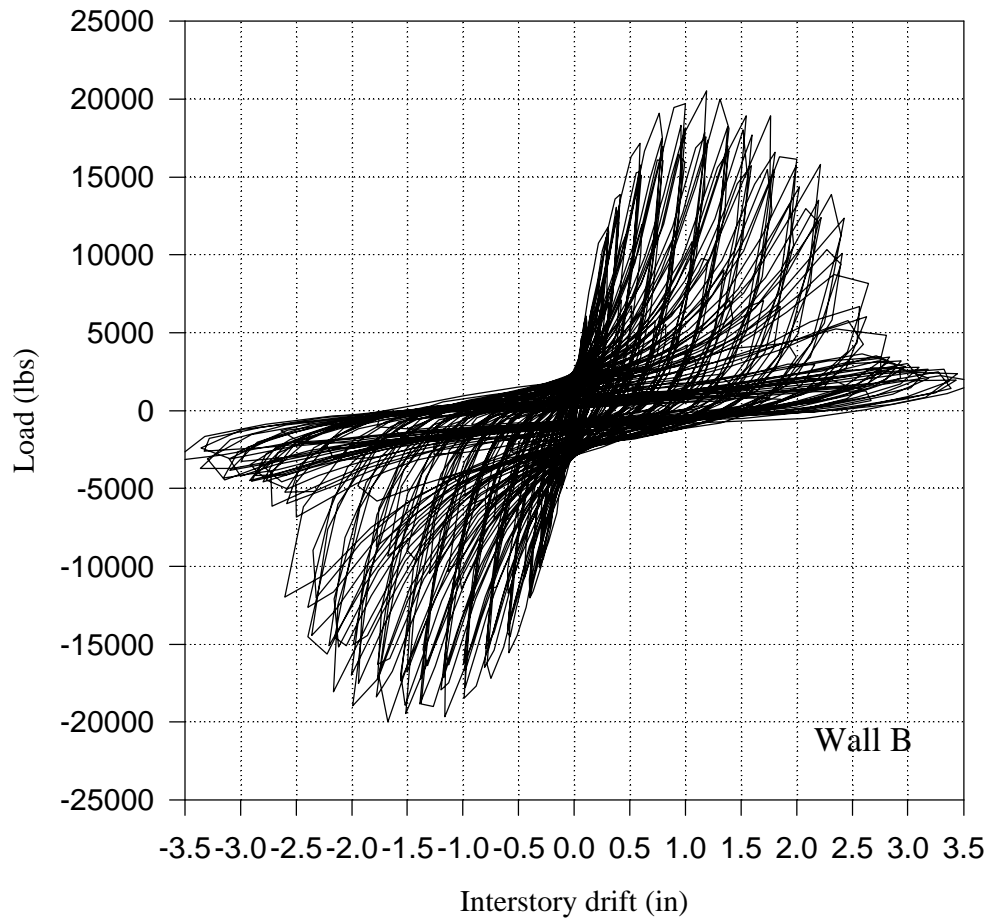
Figure A2-1: Load deflection history of Wall B (r = 0.76)
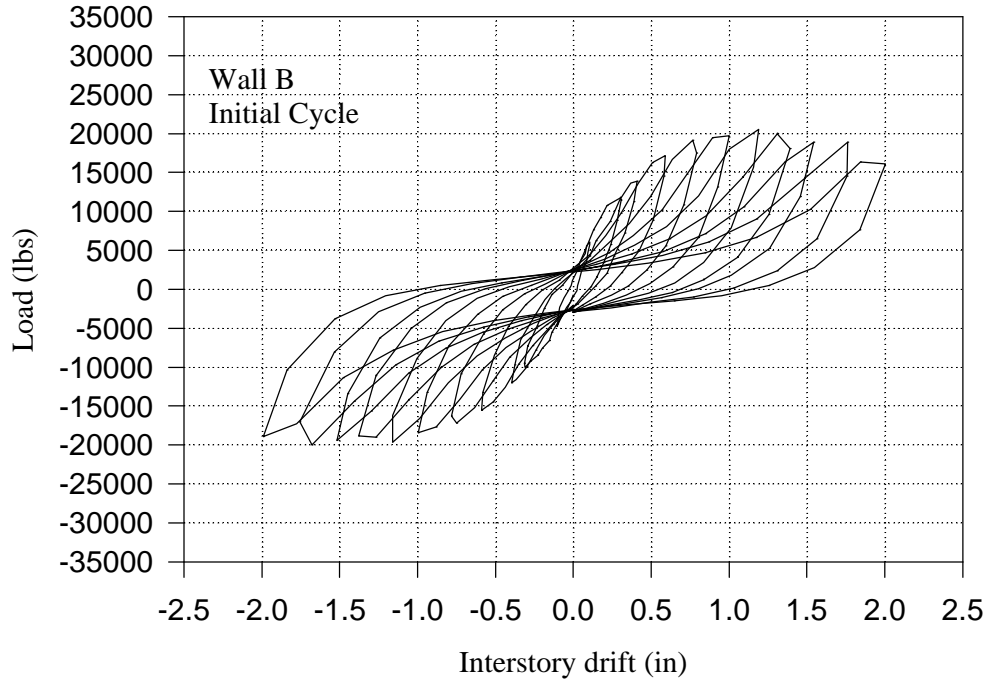
Figure A2-2: Initial cycle hysteresis loops of Wall B
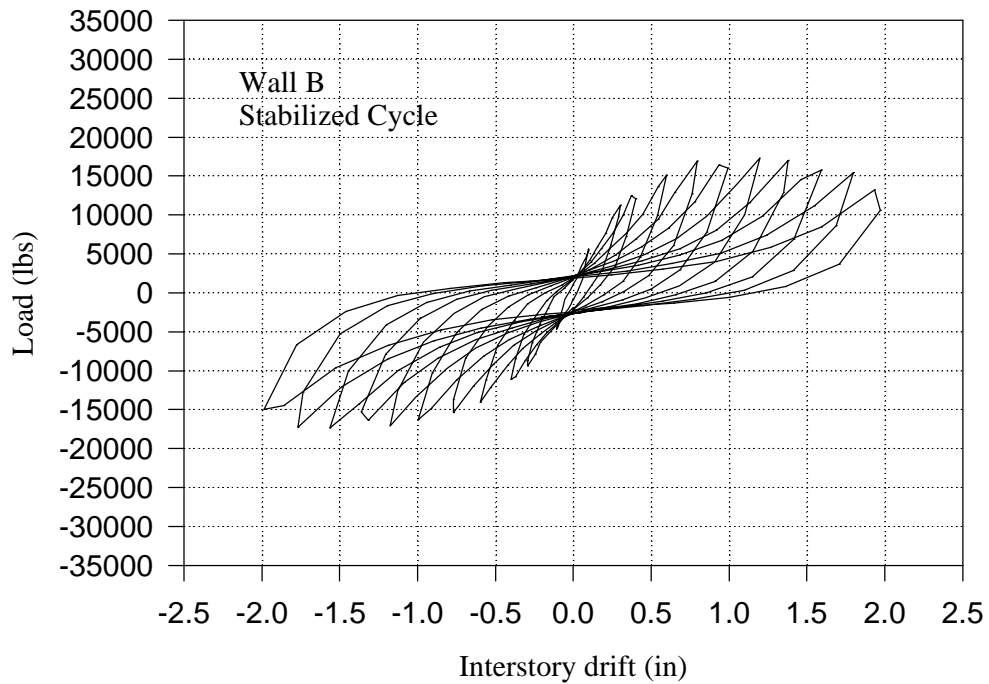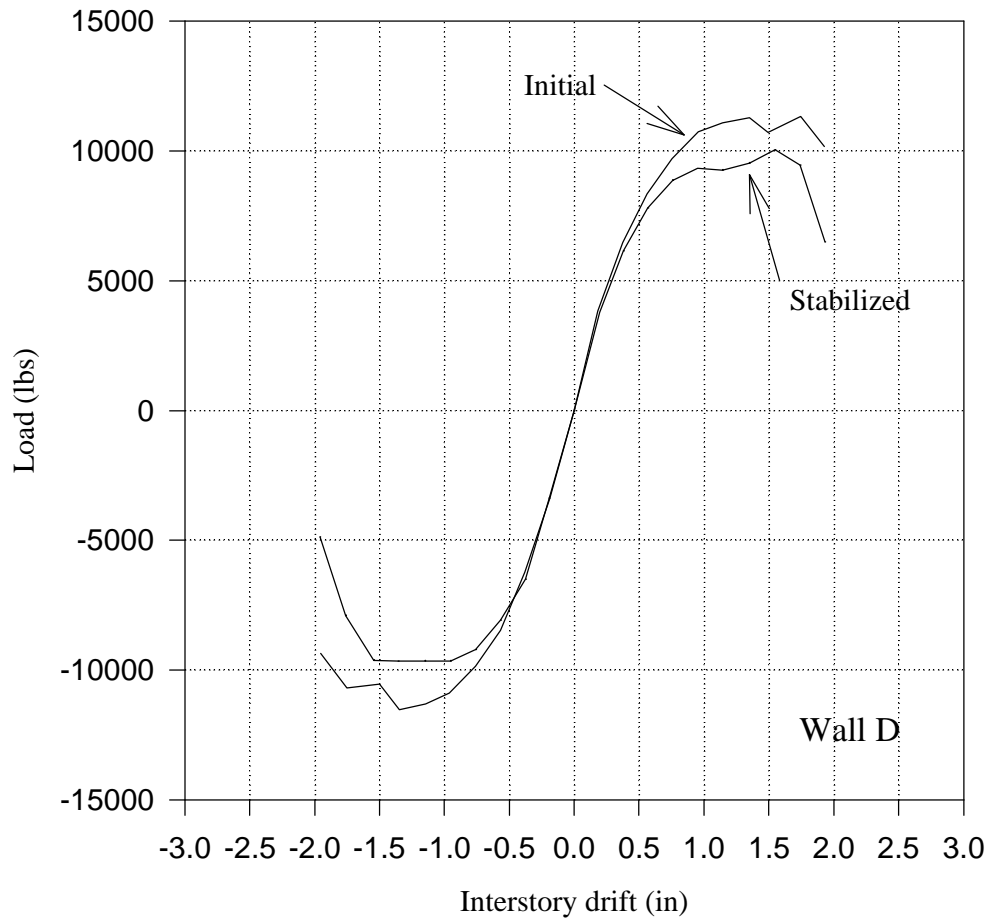

Figure A2-3: Stabilized cycle hysteresis loops of Wall B
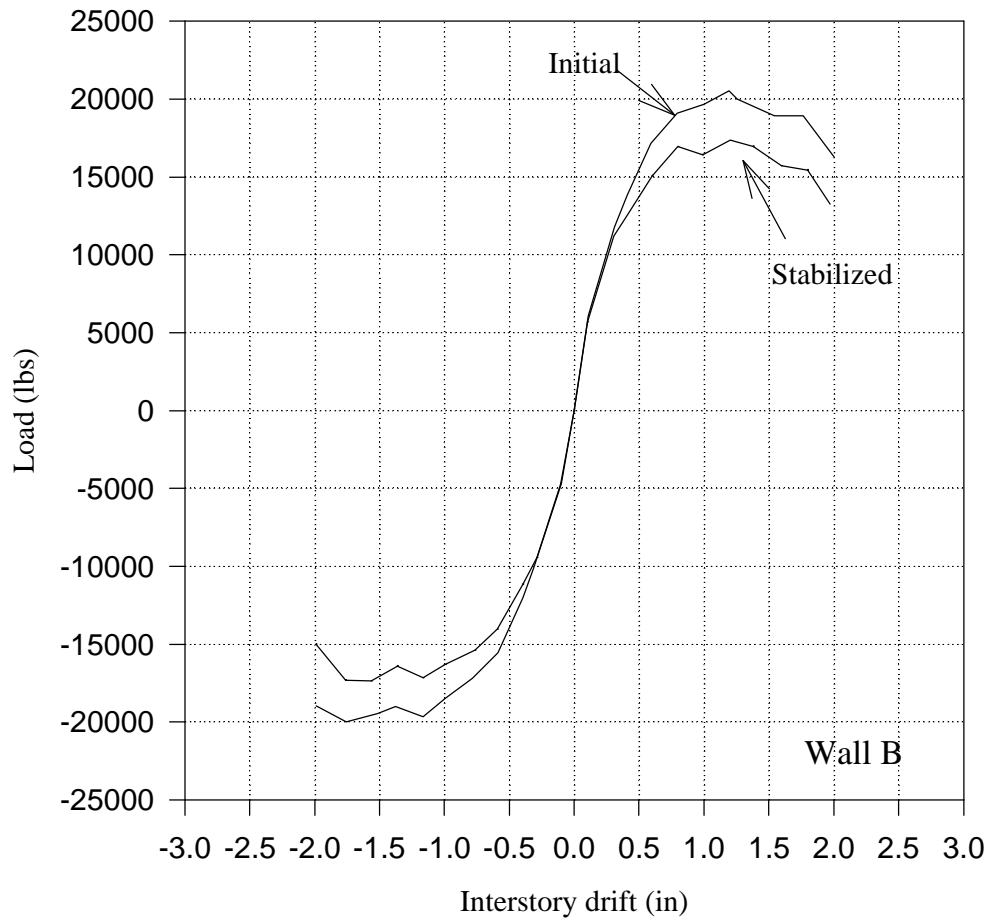
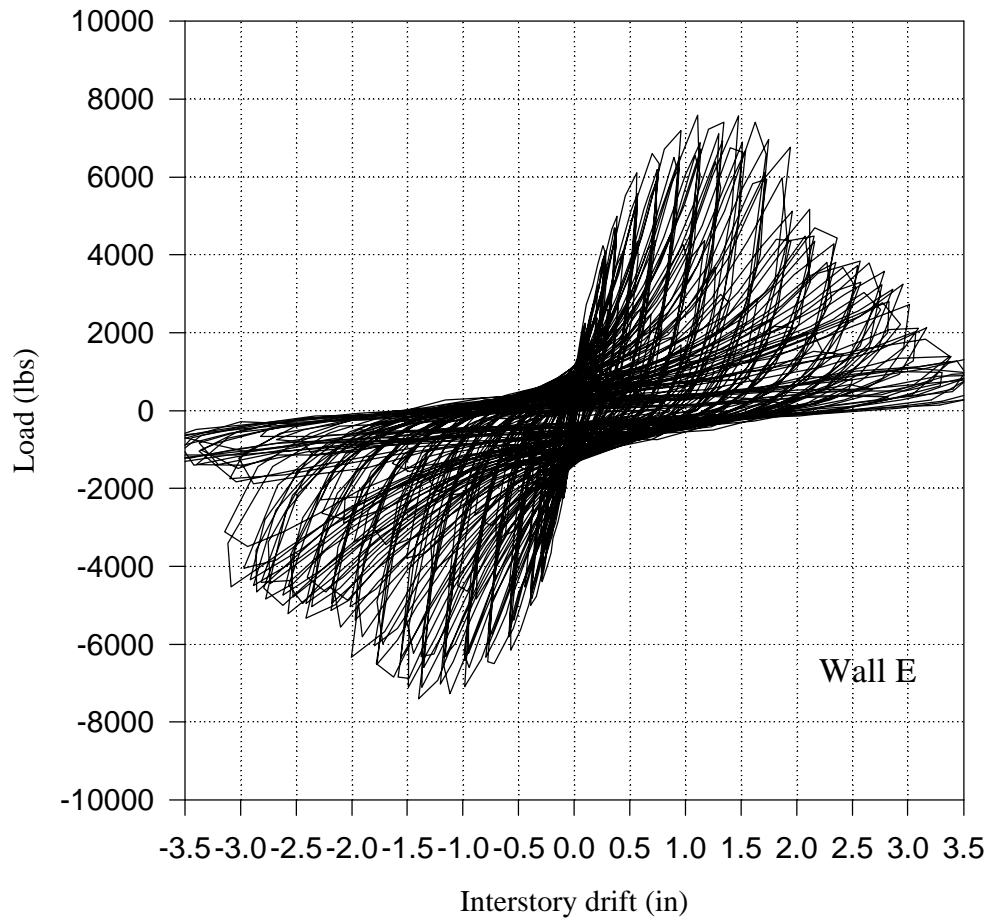**Figure A2-4: Initial and stabilized load envelope curves for Wall B (r = 0.76)**
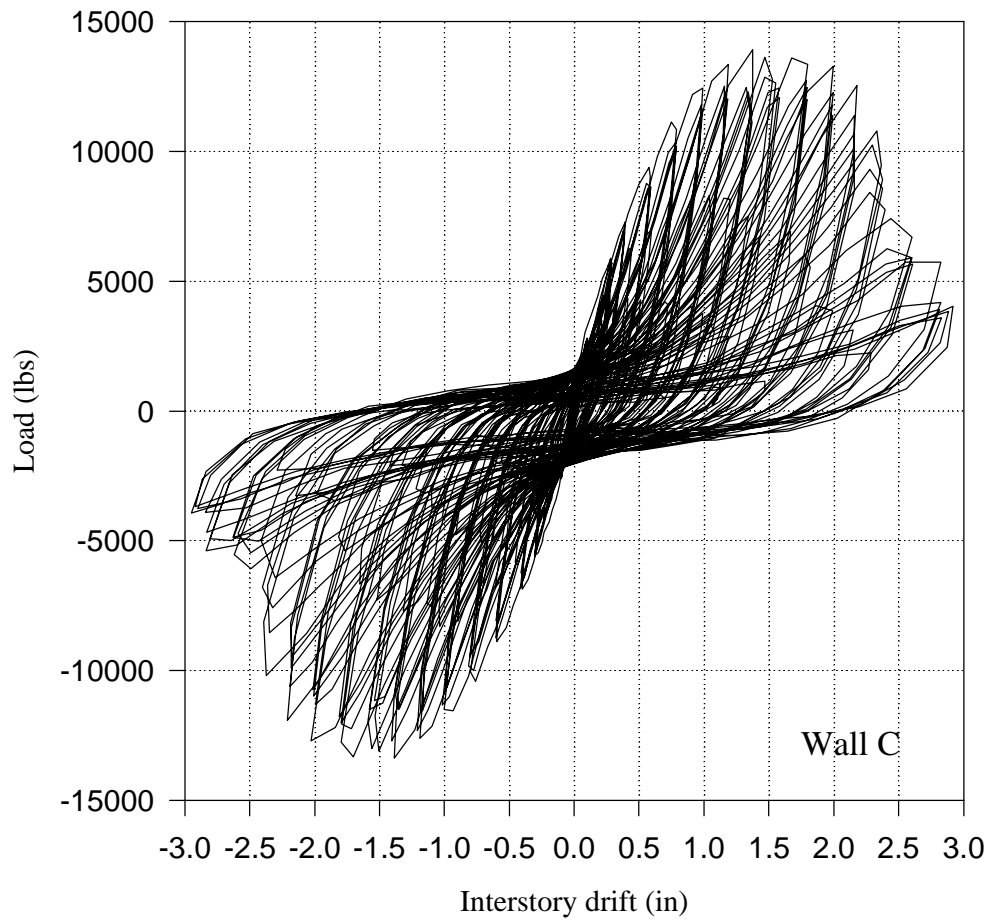
Figure A3-1: Load deflection history of Wall C (r = 0.55)
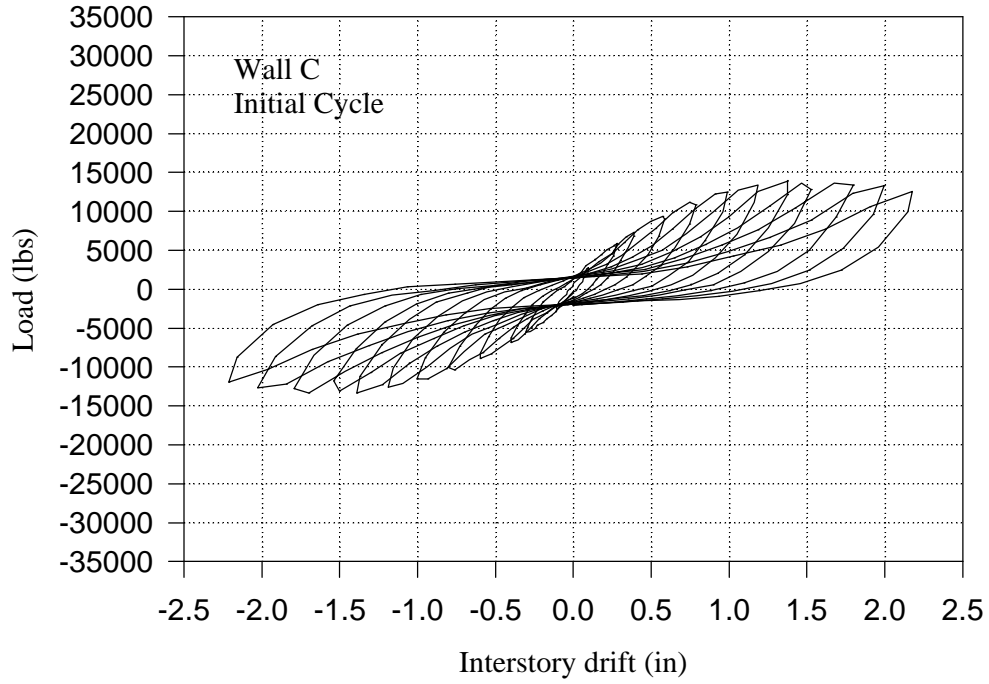
Figure A3-2: Initial cycle hysteresis loops of Wall C
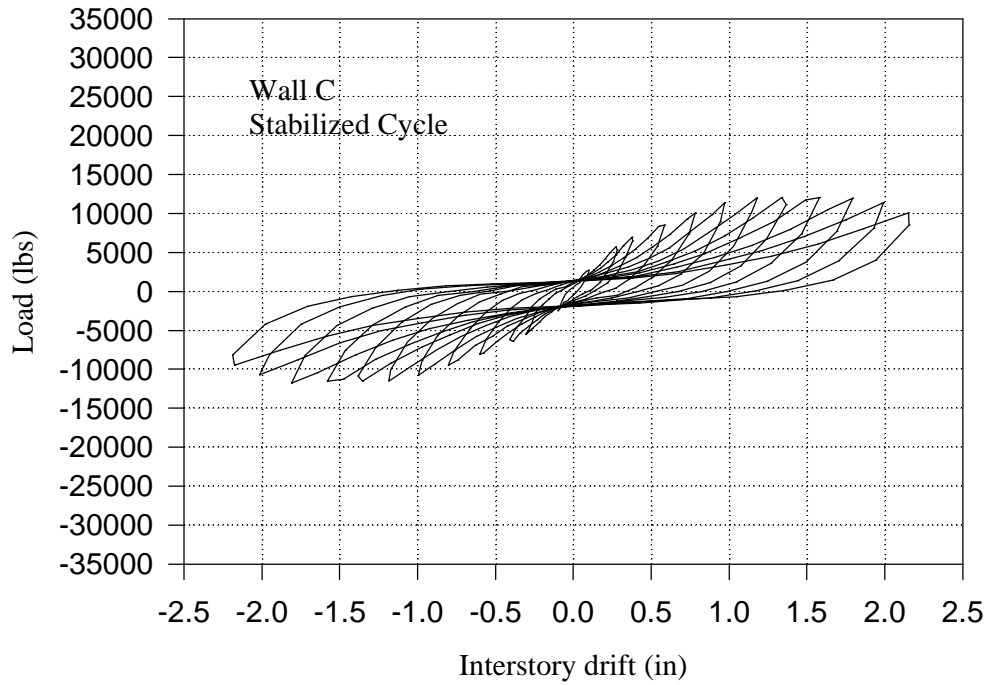
Figure A3-3: Stabilized cycle hysteresis loops of Wall C

Figure A3-4: Initial and stabilized load envelope curves for Wall C (r = 0.55)

Figure A4-1: Load-deflection history of Wall D (r = 0.48)

Figure A4-2: Initial cycle hysteresis loops of Wall D

Figure A4-3: Stabilized cycle hysteresis loops of Wall D

Figure A4-4: Initial and stabilized load envelope curves for Wall D (r = 0.48)
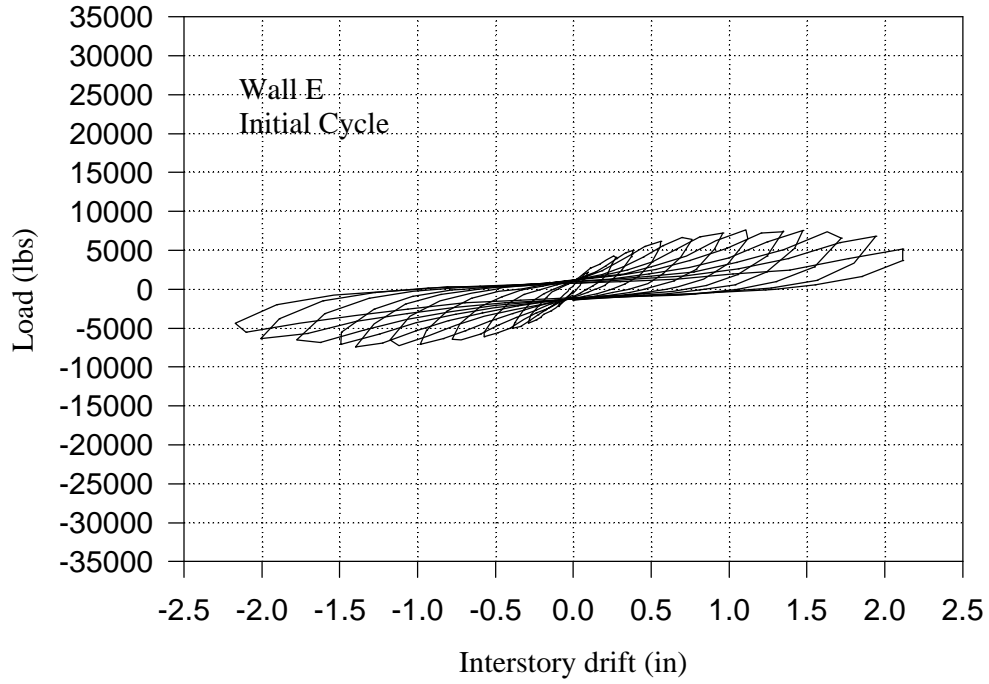
Figure A5-1: Load deflection history of Wall E (r = 0.30)
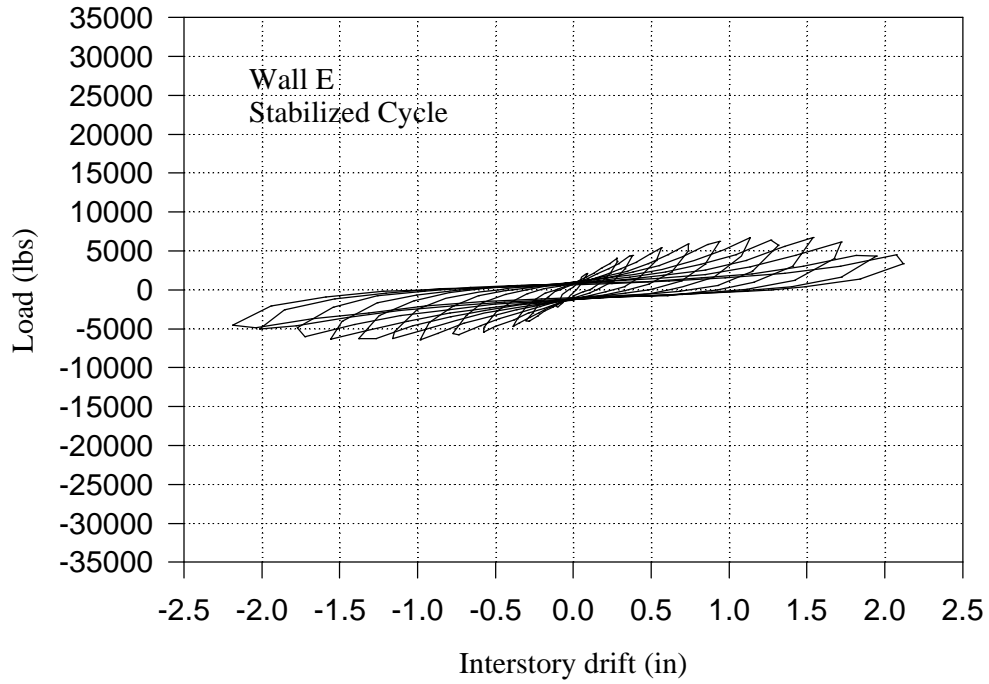
Figure A5-2: Initial cycle hysteresis loops of Wall E

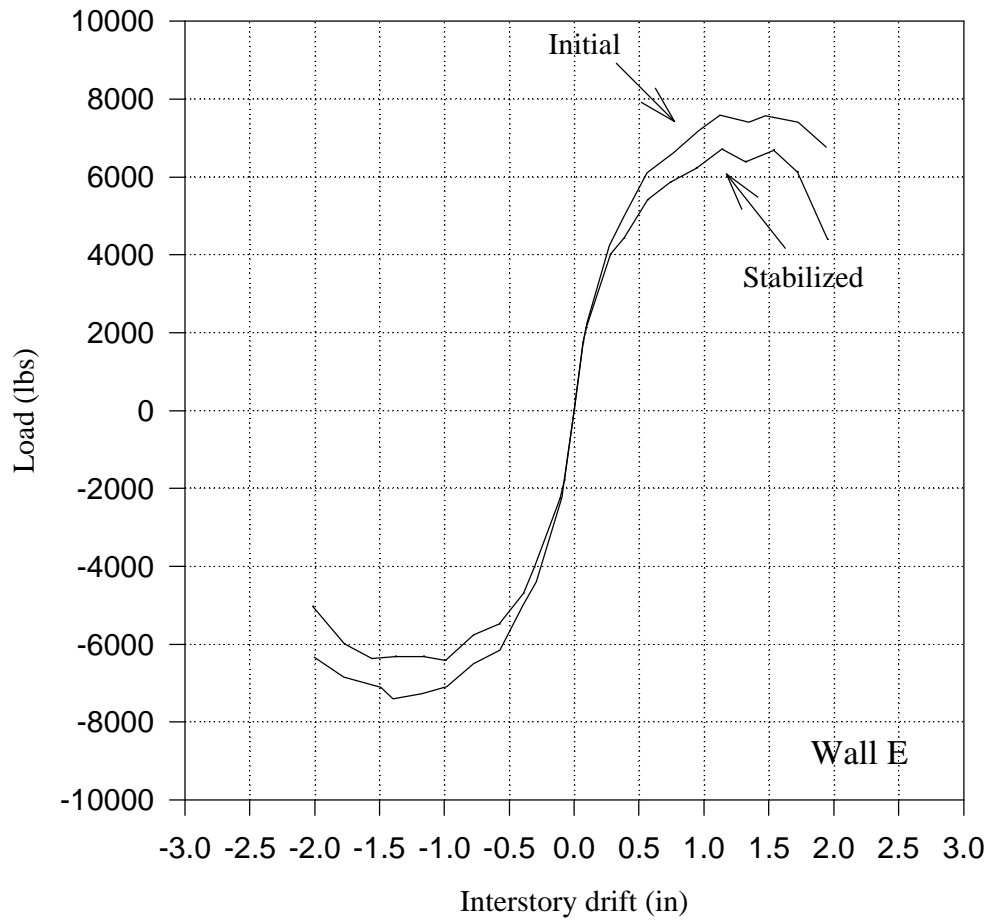**Figure A5-3: Stabilized cycle hysteresis loops of Wall E**

Figure A5-4: Initial and stabilized load envelope curves for Wall E (r = 0.30)